Intensification of hollow fiber membrane cross-flow filtration by the combination of helical baffle and oscillatory flow

Horie, Takafumi ; Shiota, Saori ; Akagi, Takaaki ; Ohmura, Naoto ; Wang, Steven ; Eze, Valentine ; Harvey, Adam ; Hirata, Yushi

(Citation)
Journal of Membrane Science,554:134-139

(Issue Date)
2018-05-15

(Resource Type)
journal article

(Version)
Accepted Manuscript

(URL)
https://hdl.handle.net/20.500.14094/90004820

Title: Intensification of hollow fiber membrane cross-flow filtration by the combination of helical baffle and oscillatory flow

Authors: Takafumi Horie[a,b]*, Saori Shiota[a], Takaaki Akagi[a], Naoto Ohmura[a], Steven Wang[c], Valentine Eze[c], Adam Harvey[c], Yushi Hirata[d]

[a] Department of Chemical Science and Engineering, Kobe University
1-1 Rokkodai, Nada, Kobe, Hyogo, 657-8501, Japan

[b] Center for Membrane and Film Technology, Graduate School of Engineering, Kobe University
1-1 Rokkodai, Nada, Kobe, Hyogo 657-8501, Japan

[c] School of Chemical Engineering and Advanced Materials, Newcastle University,
Newcastle Upon Tyne, Tyne and Wear NE1 7RU, UK

[d] Graduate School of Engineering Science, Osaka University,
1-3 Machikaneyama, Toyonaka, Osaka 560-8531, Japan

*Corresponding author

E-mail address: horie@dragon.kobe-u.ac.jp

ABSTRACT

Separation performance of ultrafiltration has been hindered by membrane fouling and concentration polarization. This study investigated the effect of fluid dynamics induced by the combination of a helical baffle and oscillatory flow on the performance of a hollow fiber membrane module. An external pressure type cross-flow filtration was employed and purification of humic acid aqueous solution was selected as a model case. Normalized permeate flux and rejection were used for evaluation and compared in the following 4 cases; control, oscillatory flow without helical baffle, helical baffle without oscillatory flow and combined condition of helical baffle and oscillatory flow, called oscillatory baffled membrane module (OBMM). As for the OBMM, the normalized permeate flux could be kept at higher level and the rejection also showed much better performance than the others. The OBMM could maintain the clean membrane surface though all the other conditions could not inhibit the humic acid accumulation. These were caused by the vortices and the swirling flow resulting in the high shear stress and the renewal of the concentration polarization layer by their mixing effect. Finally, the oscillation conditions were varied and summarized in the oscillatory Reynolds number, Re_o, and the filtration performance was increased with the rise of Re_o corresponding to the intensity of oscillation.

Keywords (5): Water purification; Mass transfer enhancement; Swirling flow; Oscillatory baffled flow; Process intensification

1. Introduction

Ultrafiltration (UF) and microfiltration (MF) hollow fiber membranes are becoming more popular in water treatment to obtain clear water because of their advantages such as superior water quality, environmentally friendly, easy control of operation, low cost and easy maintenance [1]. However, this membrane separation technology has been suffering from the problems of concentration polarization and fouling. The concentration polarization is the emergence of solute concentration gradients at a membrane and solution interface resulted from selective transfer through the membrane under the effect of transmembrane driving forces [2]. The concentration polarization layer where a higher level of solute nearest to the upstream membrane surface generates can be described by the mass balance equation [3]:

$$\frac{C_{\mathrm{m}} - C_{\mathrm{p}}}{C_{\mathrm{b}} - C_{\mathrm{p}}} = \exp(J_{\mathrm{v}}/k), \quad k = \frac{D}{\delta} \quad \cdots (1)$$

where C_{m}, C_{b} and C_{p} are the solute concentration on the membrane surface, of the bulk solution and of the permeate, respectively; J_{v} is the permeate flux and k is the mass transfer coefficient; D is the diffusion coefficient of a solute and δ is the concentration film thickness. The high concentration gradient between C_{m} and C_{p} promotes the solute to permeate through the membrane and results in the reduction of separation efficiency. Besides, the concentration gradient between the feeding and permeation sides of the membrane also causes an increase of the osmotic pressure gradient in the membrane, which reduces the permeation flux. A fouling is usually caused by the deposition of the solute on its external surfaces, at its pore openings, or within its pores due to this high concentration layer, and leads to the permeate flux reduction. The fouling also leads to the increase of the ability to reject the foulant due to the pore capacity decline or cake layer formation.

The use of high shear stress on the membrane surface has long been considered as one of the most efficient ways for increasing permeate flux [4]. The enhanced membrane shear stress generated at the membrane fluid interface results in a continuous fouling removal of the membrane surface and high

77 linear velocity leading to reduction of the concentration polarization layer. Turbulent flow can mitigate
78 the growth of the cake layer formed on the membrane. However, this is typically accompanied by high
79 axial pressure drops resulting from the large velocities which could results in a decrease of
80 transmembrane pressure (TMP) and permeation flux decline with path length. Intensification of
81 membrane filtration was reported by Gomaa *et al*. [5] about oscillation of a flat membrane.
82 Microfiltration of bakers yeast was selected as a model case. The flat membrane was fixed in the
83 filtration unit by sealing its edges, and was mechanically oscillated along its surface. The enhanced
84 membrane shear stress generated at the membrane fluid interface resulted in a continuous fouling
85 removal of the membrane surface and renewal of the mass transfer boundary layer leading to
86 significant performance improvement. In their later papers, the combined effect of using oscillations
87 and turbulence promoters (TPs) were investigated [6]. Experiments were performed using surfaces
88 equipped with both flat turbulence promoters and grooved turbulence promoters. The turbulence
89 promoters in presence of oscillations has proven effective in enhancing membrane microfiltration flux
90 and in achieving near self-cleaning conditions with low specific energy consumption.
91 Oscillatory baffled reactors (OBRs) have received considerable attention as a process
92 intensification devise to convert batch processes to continuous processes. OBRs can provide plug flow
93 behavior in the laminar flow regime by interaction between the oscillating fluid and baffles inserted
94 in the reactor tube. Also, the reactors successfully enhanced heat and mass transfer and controllable
95 mixing conditions. As for the meso-scale reactor, the bulk flow performance inside the helical baffle
96 design was compared to other mesoscale configurations, and a high degree of plug flow performance
97 could be achieved due to the swirling flow motion and vortex generation [7]. In this study, the
98 oscillatory baffled membrane module using a helical coil was employed as the potential application
99 for hollow fiber membrane cross-flow filtration processes and the effect of the oscillatory baffled flow
100 on the filtration performance and the mechanism were investigated by using dimensionless numbers.
101

2. Materials and Methods

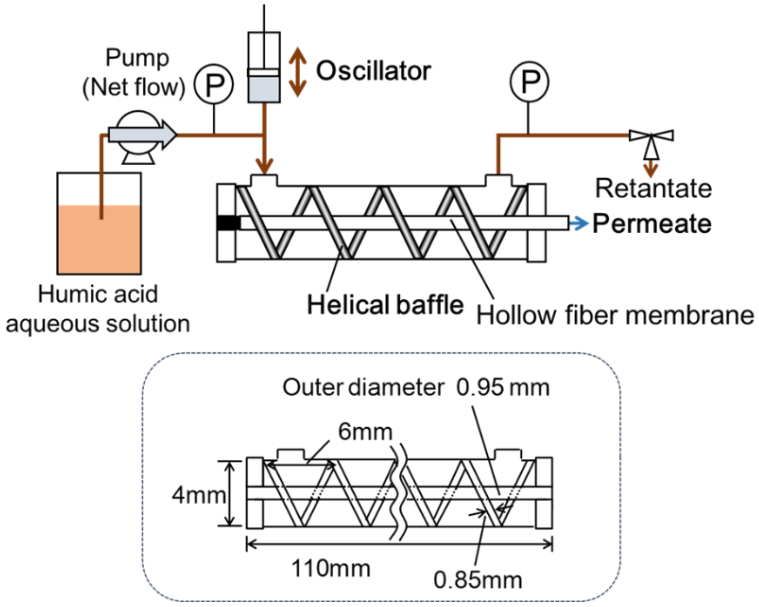

Fig.1 Schematic illustrations of the membrane module with a helical baffle insert and laboratory-scale membrane filtration apparatus with an oscillator.

Humic acid is one of the major foulants in drinking water production [8]. Its aqueous solution was employed as a model case for water purification and its concentration was fixed at 50 mg·L^{-1} (pH = 8.4). The schematic of the experimental apparatus is shown in Fig. 1. A membrane module consisted of one hollow fiber membrane (Daicen Membrane-Systems LTD. (Product No. FUS1582); Outer-diameter 0.95 mm; Inner-diameter 0.80 mm; effective surface area 3.3×10^{-4} m^2; molecular weight cut off, MWCO, 150,000 Da and 30,000 Da) made of polyethersulfone and housed concentrically in an acrylic resin cylinder with an inner-diameter of 4 mm and length of 110 mm. The humic acid aqueous solution was continuously fed into the module with a peristaltic pump at the flow rate of 0.277 mL·s^{-1}, and the purified water permeated through the membrane from the outside to the inside driven by the transmembrane pressure (TMP) 0.5 bar. A bronze helical coil with a diameter of 0.85 mm was inserted as the helical baffle in the gap between the hollow fiber and the tube. The pitch of the coil was determined to be 6 mm according to the design of meso-scale oscillatory baffled reactors reported by

127 Phan *et al*. [9]. In a typical operation of conventional OBRs, the parameter baffle open area is chosen
128 in a range of 0.2–0.4, and the baffle spacing ratio is in a range of 1.5 – 2, usually 1.5. The open area,
129 i.e. aperture ratio here, was 0.34 which was calculated by subtracting the projected areas of the
130 membrane and the helical baffle from the cross sectional area of the module. The baffle spacing ratio
131 corresponding to the pitch length for helical baffles was 1.5 (6 mm).

132 For the oscillation flow experiments, a piston syringe pump called as "oscillator" was used. The
133 piston of the oscillator moved back and forth to generate the oscillatory flow in the gap between the
134 membrane and the resin tube with the frequency, f, of 0.1 – 4.0 Hz with triangular wave motion and
135 the amplitude, oscillation volume V_o, of 0.17 – 1.67 mL. The oscillation volume indicates the volume
136 difference in the oscillator syringe piston between at the highest and the lowest position. Pressure
137 indicated by the upstream pressure gauge was oscillated in synchronization with the oscillator motion.
138 The pressure valve in the downstream of membrane was manually controlled so that the center of
139 oscillation could always be in the position of the specified transmembrane pressure.

140 The permeate flux was evaluated by the normalized permeate flux, J/J_0 where J_0 was obtained
141 based on the pure water permeate flux for each membrane to eliminate the individual membrane
142 variability. Samples permeated through the membrane and dripping out from the one side of the
143 membrane were collected and weighed to determine a permeate flux. Next, separation ability can be
144 generally expressed as:

145
$$R_{\mathrm{app}} = 1 - \frac{C_{\mathrm{p}}}{C_{\mathrm{b}}} \quad \cdots (2)$$

146
$$R_{\mathrm{int}} = 1 - \frac{C_{\mathrm{p}}}{C_{\mathrm{m}}} \quad \cdots (3)$$

147 The former description of the rejection is called as an apparent rejection factor, R_{app}, which expresses
148 the global ability of the membrane separation. The latter is the intrinsic rejection factor referring to a
149 local relationship between upstream and downstream which corresponds to the membrane ability for

150 the separation. In this study, rejection, R, which corresponded to the percentage expression of R_{app} (%)
151 was employed for the evaluation. The humic acid concentration, C_p, of samples was determined by
152 measuring absorbance at 254 nm light using a UV–vis spectrophotometer, SHIMADZU MPS-2400.
153
154 **3. Results and discussion**
155 **3.1 Comparison of the filtration performance for different operation conditions**
156 Fig. 2 shows the time course change of normalized permeate flux and rejection when the membrane
157 of MWCO 150 kDa was used. 4 conditions were compered; (C) is a control condition that no baffle
158 was used and no oscillatory flow was added, (O) is an oscillatory flow condition without a baffle, (B)
159 is a baffled condition without oscillatory flow and (OB) is a baffled condition with oscillatory flow.
160 The oscillating conditions for (O) and (OB) were identical at f = 3.3 Hz and V_o = 0.167 mL. The net
161 flow rate was identical at 0.277 mL·s^{-1} for each case, and the net flow Reynolds number was defined
162 and calculated as below.

$$Re_n = \frac{\rho u D_h}{\mu} \quad \cdots (4)$$

163
164 where u is the mean superficial flow velocity (m·s^{-1}); ρ is density (kg·m^{-3}·s^{-1}) and μ is viscosity (Pa·s).
165 D_h is the hydraulic diameter (m) which is four times of the cross-sectional area of the flow divided by
166 the wetted perimeter of the cross-section. Although Re_n was different for the baffled conditions and
167 non-baffled conditions, it was 58 and 55, respectively. We considered that the difference between them
168 was so small to be considered to play a minor role.
169 At the initial stage, every normalized permeate flux was high and rejection was low because there
170 was no foulant on the membrane and pores were not blocked at all. Subsequently the normalized
171 permeate flux decreased rapidly since the high permeate flux promoted the transportation of the humic
172 acid to the membrane surface and led to the high accumulation rate. On the other hand, the rejection
173 was increased due to pore size reduction caused by the fouling. As for the oscillatory baffled condition,

the decrease of the normalized permeate flux was relatively moderate and kept the flux at the higher value than the others. It was 0.43 and 90% which was about 1.5 times higher than the others. This is because the interaction between the helical baffle and oscillatory flow generated vortices around the membrane surface and the vortices caused the high shear stress removing the foulant. Contrary to the

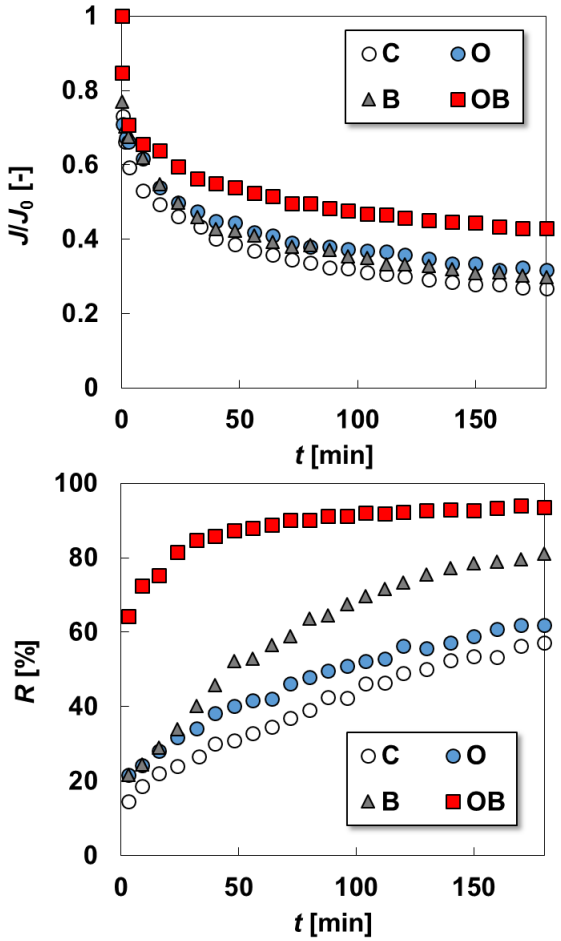

Fig.2 Comparison of the time course change of (a) the normalized permeate flux, J/J_0, and (b) the rejection, R, during filtration using a PES membrane of MWCO = 150 kDa for (C) the control condition no baffle and no oscillatory flow, (O) oscillatory flow condition without a baffle, (B) baffled condition without an oscillatory flow and (OB) oscillatory baffled flow. The oscillating conditions for (O) and (OB) were identical at f = 3.3 Hz and V_o = 0.167 mL.

199 reduction of the foulant accumulation, the rejection could be maintained higher than the others. The
200 helical baffle was a guide to generate the swirling motion of the fluid flow in the module [10]. The
201 generation of the swirling flow in the oscillatory baffled reactor with a helical baffle was reported by
202 Salano *et al*. [11] though there was no membrane in the center of the module. The swirling motion has
203 the similar trajectory as the helical baffle configuration and it assumed to create a streamline in the
204 tangential direction from the membrane surface. This flow motion prevented the foulant from
205 approaching to the surface, and the concentration increase at the vicinity of the surface was suppressed
206 as well. It could be observed that the baffled condition without an oscillatory flow showed the higher
207 rejection than the cases of control and oscillatory motion without a baffle due to the foulant approach
208 prevention. However, the permeate flux reduction could not be avoided since the high shear stress
209 caused by the vortex motion was not generated in these cases.
210 The outside views of the membrane surfaces were compared for the above 4 cases in Fig. 3. The
211 control condition couldn't inhibit the humic acid accumulation and its surface became brown, color of
212 humic acid, overall. In the case of the oscillatory flow, it was reported that superimposing an oscillating
213 onto bulk axial flow in a tube produced a higher velocity profile nearer the wall than the center-line
214 [12], but the improvement was little and the color of the surface was slightly and partially
215
216
217
218
219
220

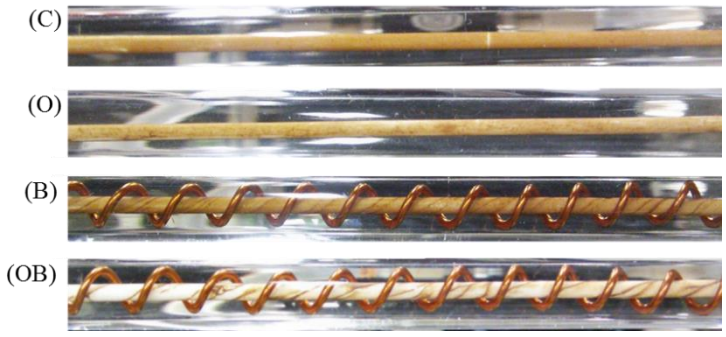

221 Fig.3 Photographic images of the PES membrane surfaces (MWCO = 150 kDa) fouled by humic
222 acid after 180 min filtration operation in order to compare (C), (O), (B) and (OB) conditions.
223

lighter than the control. As for the baffled condition without an oscillatory flow, the color of the surface was brown and almost the same as the control, but the spiral trace of fouling could be observed. In our previous paper [10], the streamlines in this module were numerically simulated, and they showed spiral trajectories along the helical baffle. This swirling fluid motion caused the spiral trace of fouling. As for the oscillatory baffled condition, the color of the surface was kept to be white, original color of membrane, and the spiral trace of fouling could be observed as well. Obviously the inhibition of fouling was achieved due to the vortices and the swirling flow generated along the baffle.

Fig. 4 shows the time course change of normalized permeate flux and rejection when the membrane of MWCO 30 kDa was used. The operation condition was the same as Fig. 2, but the pore size was smaller, and thus the net permeate flux was much lower than the above. For the case of (C), the normalized permeate flux and rejection were lower than the other 2 cases. In Fig. 5 (C), surface fouling occurred on the overall membrane surface although the color of the surface was lighter than the one in Fig.3. This covered surface overall was the main cause of the permeate flux reduction. As for the baffled condition (B), even just the swirling flow generating the streamline in the tangential direction to the membrane surface could disturb the concentration polarization layer and prevent the formation of the fouling layer under the lower permeate flux condition. Thus, the normalized permeate flux and rejection became higher than the control condition. However, in Fig. 5 (B) the effect of the flow in the tangential direction appeared locally and the fouling was observed on the membrane with the spiral trace along the helical baffle. Although the local fouling was darker than the control, it is considered that the higher permeate flux was attributed to the partially clear area. As for the oscillatory baffled condition (OB), the normalized permeate flux and rejection improved more than the baffled condition without an oscillatory flow, and the very clear membrane surface could be observed in the picture of Fig. 5 (OB). This is because the generation of the vortex motion intensify not only the flow in the tangential direction but also the shear stress. As a result, the normalized permeate flux was more than twice as the control and the rejection reached close to 100%.

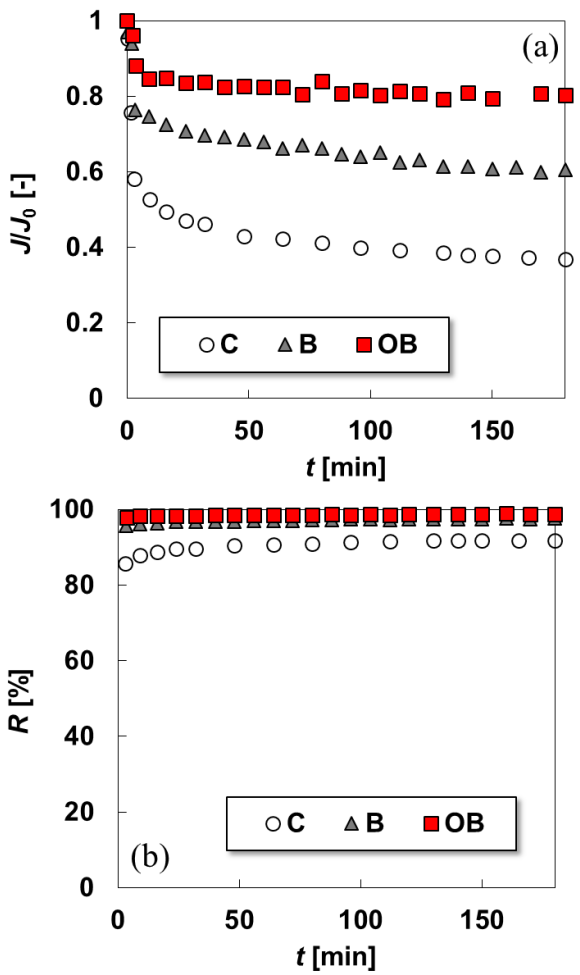

Fig.4 Comparison of the time course change of (a) the normalized permeate flux, J/J_0, and (b) the rejection, R, during filtration using a PES membrane of MWCO = 30 kDa for (C), (B) and (OB) at f = 3.3 Hz and V_o = 0.167 mL.

Fig.5 Photographic images of the PES membrane surfaces (MWCO = 30 kDa) fouled by a humic acid after 180 min filtration operation in order to compare (C), (B) and (OB) conditions.

When comparing two membranes with distinctive cut-offs, 150 and 30 kDa. Fouling mitigation was more successful in the case of 30 kDa membrane. The mechanism of the fouling was confirmed to be cake formation on the membrane surface by the model fitting in our previous paper [10]. However, the fouling models cannot be distinguished perfectly, and some of the foulant absorbed on the membrane pore walls to reduce the permeate flux. In the case of 30 kDa, the pore size is much smaller than the 150 kDa. The cake formation was more dominant than the case of 150 kDa. Furthermore, the permeate flux was much lower than the case of 150 kDa, and the accumulation rate of foulant became much slower due to the lower transportation of the solute to the membrane surface. Therefore, the effect of the fluid motion in the case of 30 kDa became more significant to remove the fouling and disturb the concentration polarization layer.

3.2 Effect of oscillatory conditions on the filtration performance

Fig. 6 shows the outside views of the membrane surface at various oscillatory conditions after 3 hours operation. The left pictures are arranged in ascending order of the frequency and the right ones are in ascending order of the oscillating volume. The frequency and the oscillating volume indicates how large the oscillating velocity was and the amplitude of the oscillation was, respectively. The larger

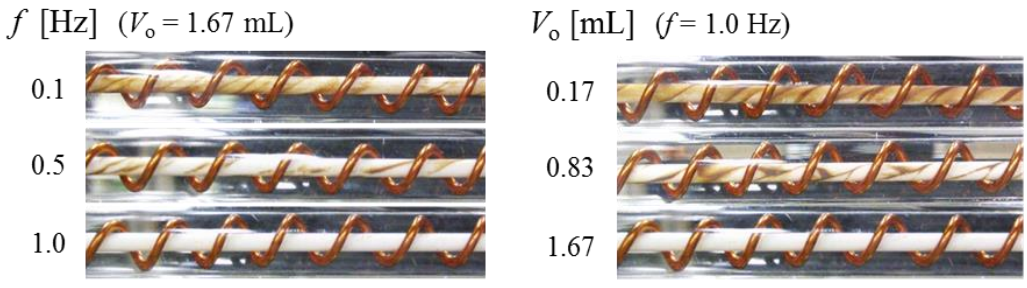

Fig.6 Photographic images of the PES membrane surfaces (MWCO = 150 kDa) fouled by a humic acid after 180 min filtration operation at the various oscillating conditions (left column) frequency, f, and (right column) oscillating volume, V_o.

299 frequency and oscillating volume became, the more fouling was suppressed. At f = 1.0 Hz and V_o =
300 1.67 mL, the surface was white and foulants could be hardly observed on the membrane surface.
301 The fluid mechanics in the module can be described by two dimensionless groups, which were
302 reported by Brunold *et al*. [13] who followed Sobey's examples and definitions [14], referring the first
303 group as the oscillatory Reynolds number, Re_o for conventional OBRs. The flow conditions can be
304 presented as

$$Re_o = \frac{\rho u_p D_t}{\mu} \quad \cdots (5)$$

305

306 and the second group as the Strouhal number

$$St = \frac{\omega D_t}{4\pi u_p} \quad \cdots (6)$$

307

308 where u_p is the pulsating velocity (m·s^{-1}); D_t is the tube diameter (m); ω is the angular frequency of
309 oscillation (rad·s^{-1}). The oscillatory Reynolds number (Re_o) describes the intensity of mixing inside a
310 column, reactor or module. The Strouhal number is a measure of the effective eddy propagation. If it
311 is too high the vortices will be propagated into the next baffle cavity [15]. The oscillatory Reynolds
312 number and Strouhal number were modified for the membrane module and triangular wave motion as

$$Re_o = \frac{\rho(2fV_o/S)D_h}{\mu} = \frac{4fx_o\rho D_h}{\mu} \quad \cdots (7)$$

313

$$St = \frac{2\pi f D_h}{4\pi(2fV_o/S)} = \frac{D_h}{8x_o} \quad \cdots (8)$$

314

315 where S is the cross-sectional area (m^2) and D_h is the hydraulic diameter (m) defined in Eq.(2); f is the
316 frequency of oscillation (Hz) and x_o is the center-to-peak amplitude of oscillation (m) corresponding
317 to $V_o/(2S)$. In Fig. 7, the normalized permeate flux and the rejection for MWCO 150 kDa membrane
318 at 180 min obtained under the various oscillation conditions were summarized against the oscillatory
319 Reynolds number, Re_o. Both of them were correlated with Re_o or increased with the increment of Re_o,

and almost identical values could be obtained at the same Re_o even when the amplitude and frequency were different. Therefore, the high intensity of the mixing by the vortex motion inside of the module removed the fouling and prevented the concentration polarization effectively. Meanwhile, against the Strouhal number in Fig. 8 the normalized permeate flux and rejection were increased sharply and had the peak at 0.05. Over 0.05, the both of the performances were settled to the constant value along with the increase of *St*. It means that the effect of vortex propagation worked effectively around 0.05 and more effects of the vortex propagation could not be obtained over the value.

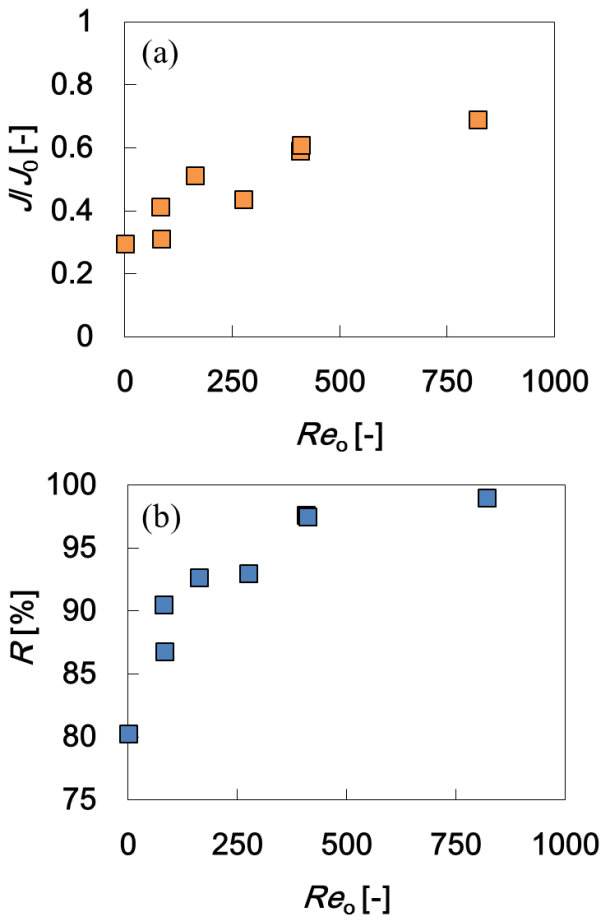

Fig.7 Influence of oscillatory Reynolds number on (a) the normalized permeate flux and (b) the rejection after the 180 min filtration operation for the membrane with MWCO 150 kDa

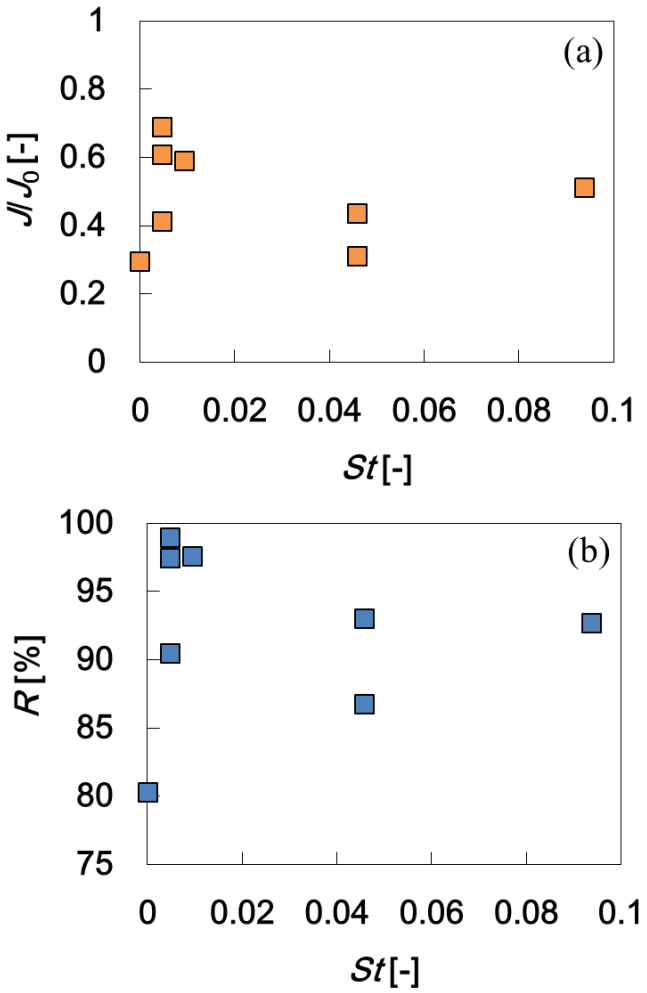

Fig.8 Influence of Strouhal number on (a) the normalized permeate flux and (b) the rejection after the 180 min filtration operation for the membrane with MWCO 150 kDa.

The highest results of normalized permeate flux and rejection were 0.69 and 99%, respectively as far as they were restricted in the conditions of this study. The normalized permeate flux 0.69 was almost doubled compared to the control and the reduced performance from the initial state was only 0.31. Moreover, the rejection was almost 100 % could be achieved only by using the fluid motions under the laminar flow regime. The filtration performance was improved significantly, but the evaluation of the energy consumption couldn't have been yet to be implemented, and there is no equation in the literature which can estimate the energy dissipation of OBR with helical baffle though

there exists the equation for conventional oscillatory baffled reactors (with orifice-type baffles) [16]. The further investigation for the energy dissipation is needed for the module to be in practical use.

4. Conclusions

This study investigated the intensification of the filtration performance with the hollow fiber membrane module utilizing the combination of the helical baffle and the oscillatory flow. The helical baffle generated the swirling flow resulting in the tangential direction flow from the membrane surface. This could suppress the approach of the humic acid to the membrane surface and reduce the concentration polarization effect. When the oscillation was added to the upstream flow, the vortices appeared between the baffle and enhanced the tangential direction flow for the renewal of the concentration polarization layer and the shear stress at the membrane surface for the removal of the fouling. As a result, higher permeate flux and rejection could be achieved than the other three conditions. The frequency and amplitude were varied and summarized in Re_o, which indicated the intensity of mixing in the module, and thus the permeate flux and rejection drastically increased with the increase of Re_o. In addition, they showed the optimum value around $St = 0.05$, which indicated that the effect of vortex propagation worked effectively around 0.05. At the optimum operation condition, the normalized permeate flux of 0.69 and the rejection of 99% could be achieved while 0.30 and 80% for the baffled condition without the oscillatory flow.

Acknowledgement

This work was partially supported by JSPS KAKENHI, Grant-in-Aid for Young Scientists (B), Grant No. 16K21161. The authors also thank Mr. Kumagai for his technical support.

393 **References**

394 [1] J.G. Jacangelo, C.A. Buckley, Microfiltration, in: J. Mallevialle, P.E. Odendaal, M.R. Wiesner
395 (Eds.), Water Treatment Membrane Processes, McGraw-Hill, New York, 1996, pp. 11.1–11.39.
396 [2] E.M.V. Hoek, M. Guiver, V. Nikonenko, V.V. Tarabara, A.L. Zydney, Membrane Terminology, in:
397 E.M.V. Hoek, V.V. Tarabara (Eds.), Encyclopedia of Membrane Science and Technology, Wiley,
398 Hoboken, NJ, 2013, Vol. 3, pp. 2219–2228.
399 [3] I. Sutzkover-Gutman, D. Hasson, R. Semiat, Humic substances fouling in ultrafiltration processes,
400 *Desalination* **261** (2010) 218–231
401 doi:10.1016/j.desal.2010.05.008
402 [4] A.S. Jönsson, Influence of shear rate on the flux during ultrafiltration of colloidal substances, *J.*
403 *Membr. Sci.* **79** (1993) 93–99
404 doi:10.1016/0376-7388(93)85020-W
405 [5] H.G. Gomaaa, S. Rao, A.M. Al-Taweel, Intensification of membrane microfiltration using
406 oscillatory motion, *Sep. Purif. Technol.* **78** (2011) 336–344
407 doi:10.1016/j.seppur.2011.01.007
408 [6] H.G. Gomaa, S. Rao, M.Al Taweel, Flux enhancement using oscillatory motion and turbulence
409 promoters, *J. Membr. Sci.* **381** (2011) 64–73
410 doi:10.1016/j.memsci.2011.07.014
411 [7] A.N. Phan, A. Harvey, Development and evaluation of novel designs of continuous mesoscale
412 oscillatory baffled reactors, *Chem. Eng. J.* **159** (2010) 212–219
413 doi:10.1016/j.cej.2010.02.059
414 [8] Y. Hao, A. Moriya, T. Maruyama, Y. Ohmukai, H. Matsuyama, Effect of metal ions on humic acid
415 fouling of hollow fiber ultrafiltration membrane, *J. Membr. Sci.* **376** (2011) 247–253
416 doi:10.1016/j.memsci.2011.04.035
417 [9] A.N. Phan, A. Harvey, Effect of geometrical parameters on fluid mixing in novel mesoscale

418 oscillatory helical baffled designs, *Chem. Eng. J.* **169** (2011) 339–347
419 doi:10.1016/j.cej.2011.03.026
420 [10] T. Akagi, T. Horie, H. Masuda, K. Matsuda, H. Matsumoto, N. Ohmura, Y. Hirata, Improvement
421 of separation performance by fluid motion in the membrane module with a helical baffle, *Sep.*
422 *Purif. Technol.* (2017) In Press
423 doi: 10.1016/j.seppur.2017.07.012
424 [11] J.P. Solano, R. Herrero, S. Espín, A.N. Phan, A.P. Harvey, Numerical study of the flow pattern
425 and heat transfer enhancement in oscillatory baffled reactors with helical coil inserts, *Chem. Eng.*
426 *Res. Des.* **90** (2012) 732-742
427 doi:10.1016/j.cherd.2012.03.017
428 [12] H.B. Winzeler, G. Belfort, Enhanced performance for pressure-driven membrane processes: the
429 argument for fluid instabilities, *J. Membr. Sci.* **80** (1993) 35-47
430 doi:10.1016/0376-7388(93)85130-O
431 [13] C.R. Brunold, J.C.B. Hunns, M.R. Mackley, J.W. Thompson, Experimental observations on flow
432 patterns and energy losses for oscillatory flows in ducts with sharp edges, *Chem. Eng. Sci.* **44**
433 (1989) 1227-1244.
434 doi:10.1016/0009-2509(89)87022-8
435 [14] I.J. Sobey, Observation of waves during oscillatory channel flow, *J. Fluid Mech.*, **151** (1985) 395-
436 426.
437 doi:10.1017/S0022112085001021
438 [15] A.N. Phan, A.P. Harvey, Characterisation of mesoscale oscillatory helical baffled reactor -
439 Experimental approach, *Chem. Eng. J.* **180** (2012) 229-236
440 doi:10.1016/j.cej.2011.11.018
441 [16] J.R. McDonough, A.N. Phan, A.P. Harvey, Rapid process development using oscillatory baffled
442 mesoreactors – A state-of-the-art review, *Chem. Eng. J.* **265** (2015) 110-121

443 doi: 10.1016/j.cej.2014.10.113

444

445